

Viscoelastic Properties of Polymer Solutions in High-Viscosity Solvents and Limiting High-Frequency Behavior.

II. Branched Polystyrenes with Star and Comb Structures¹

Jacobus W. M. Noordermeer, Ole Kramer, F. Henry M. Nestler, John L. Schrag, and John D. Ferry*

Department of Chemistry, University of Wisconsin, Madison, Wisconsin 53706.
Received April 7, 1975

ABSTRACT: The storage (G') and loss (G'') shear moduli were measured for dilute solutions of star- and comb-shaped polystyrenes in Aroclor 1254 with the modified Birnboim transducer. The samples investigated were a 4-arm star of molecular weight $\bar{M}_w = 8.58 \times 10^5$, a 9-arm star with $\bar{M}_w = 5 \times 10^6$, and a 24-branch comb with $\bar{M}_w = 1.38 \times 10^6$. The range of concentration (c) was 1.3×10^{-2} to 5×10^{-2} g/ml and the temperatures were between 7.2 and 46.0°. The frequency range was 0.25 to 630 Hz. Data at different temperatures for G' and $G'' - \omega\eta_s$, where ω is the radian frequency and η_s the solvent viscosity, were successfully combined by the method of reduced variables with a reference temperature of 25°. A comparison with former data on linear polystyrenes shows that all limiting values of the dynamic viscosity at high frequency, η'_∞ , can be described by the equation $\ln(\eta'_\infty/\eta_s) = [\eta']_\infty c$ over the whole range of concentration, where $[\eta']_\infty$ is a constant independent of molecular weight and the type and extent of branching. For the star-shaped samples, the frequency dependence of G' and G'' could be described by a modification of the Peterlin internal viscosity theory appropriate for star-shaped polymers.

Several extensive studies of the dynamic viscoelastic properties of linear polystyrenes, dissolved in high-viscosity solvents, have already been reported from this laboratory.^{2,3} It has been shown that, in contradiction to the predictions of the Rouse–Zimm model theories,⁴ the real part of the dynamic viscosity, η' , approaches a finite limiting value η'_∞ at high frequencies, which is higher than that of the solvent.

In the preceding paper of this series,³ hereafter referred to as I, it was shown that for linear polymer samples no influence of the molecular weight on η'_∞ could be observed. The latter quantity only depends on the concentration of the solution. This agrees with the concept that viscoelastic measurements at high frequencies provide information about the short range internal dynamics of the polymer chain. One may expect that at these frequencies the actual length and overall shape of the polymer molecules does not play a role of importance. Only the type of polymer has an influence, as was shown by differences in η'_∞ for polystyrene and poly(α -methylstyrene).³ However, no studies have yet been made concerning the influence of branching on the high-frequency viscoelastic behavior of polymers.

In this paper, results obtained on solutions of various branched polystyrenes in highly viscous chlorinated diphenyl are described. By comparing data on linear and branched polymers, additional insight is gained into the physical mechanism underlying the high-frequency dynamic viscosity of polymer solutions.

Experimental Section

Three samples of branched polystyrene were investigated. Sample LS-13 was obtained from Professor S. Onogi of Kyoto University, Japan. It has the shape of a 4-arm star with a weight-average molecular weight \bar{M}_w of 8.58×10^5 . Sample M5E, obtained from Dr. J.-G. Zilliox of the Centre de Recherches sur les Macromolécules, Strasbourg, France, has the shape of a 9-arm star with a \bar{M}_w of 5×10^6 . Sample KI-2 was obtained from Professor M. Nagasawa of Nagoya University, Japan. It resembles a comb, with a narrow molecular weight distribution backbone and on the average 24 narrow molecular weight distribution branches randomly attached to the backbone. Its weight-average molecular weight, after fractionation, was 1.38×10^6 . Because of the randomness of the branching the morphology of this sample is not well defined.

The samples were dissolved in Aroclor 1254, lot D-612, by heating at 60° for about 3 weeks with occasional stirring. The concentrations of the solutions are given in Table I.

Storage (G') and loss (G'') moduli were measured for the solu-

tions with the modified Birnboim transducer, equipped with a computerized on-line data acquisition and processing system as described elsewhere.⁵ The frequency range was 0.25 to 630 Hz. Measurements were usually performed at 5° intervals; the maximum range was from 7.2 to 46.0°. The viscosity of the Aroclor solvent ranged from 17,400 P at 7.2° to 2.11 P at 46.0°.

Results

Storage and Loss Moduli. All data obtained by measurements at various temperatures were reduced to 25° by means of the method of reduced variables.⁴ For this purpose the reduced storage modulus $G'_p = (\rho_0 T_0 / \rho T) G'$ and the reduced loss modulus $(G'' - \omega\eta_s)_p = (\rho_0 T_0 / \rho T)(G'' - \omega\eta_s)$ are plotted against the reduced radian frequency ωa_T with logarithmic scales; ρ and T are the density of the solution and the absolute temperature, respectively, at which the measurements were made; the subscript zero refers to the standard temperature of 25°, and η_s is the viscosity of the solvent. The shift factor a_T can be calculated from the viscosity of the solution at the limit of small ω as $\rho_0 T_0(\eta - \eta_s)/\rho T(\eta - \eta_s)_0$. For the lower temperatures, where no direct data on η were available, a_T was determined from an empirical shift along the $\log \omega$ axis. The dependence of the shift factor on temperature was essentially the same for all samples at these low concentrations.

Figure 1 shows the data for a solution of sample LS-13 with a concentration of 2.69×10^{-2} g/ml. This figure closely resembles that for a linear polystyrene with $\bar{M}_w = 2.67 \times 10^5$, as shown in I. At the inflection point between the terminal (low frequency) zone and the intermediate frequency region, however, a slight bump is observed, characteristic for star polymers.^{6–8} From the data in the terminal zone the steady flow viscosity η and the steady-state compliance J_e^0 of the solution may be calculated as

$$\eta = \lim_{\omega \rightarrow 0} G''/\omega$$

and

$$J_e^0 = \lim_{\omega \rightarrow 0} G'/\omega^2 \eta^2$$

The results are given in Table I. At high frequencies the slope of $\log(G'' - \omega\eta_s)_p$ against $\log \omega a_T$ becomes unity again, indicating that $\eta'_\infty \neq \eta_s$. Values of η'_∞ are also given in Table I.

Figure 2 shows the results for a solution of sample M5E, with a concentration of 1.52×10^{-2} . Because of the higher

Table I
Parameters at Low and High Frequencies, Reduced to 25°, for Star- and Comb-Shaped
Polystyrenes in Aroclor 1254

	Sample ($\bar{M}_w \times 10^{-3}$)								
	LS-13 (858)			M5E (5000)			KI-2 (1380)		
$c \times 10^2$, g/ml	1.81	2.69	3.54	1.52	3.12	5.00	1.34	2.73	3.25
η , P	423	700	1297	690	2577	10569	229	548	760
$\log J_e^0$	-3.65	-3.67	-3.72	-2.99	-3.26	-3.40	-3.57	-3.48	-3.51
$[\eta/(\eta - \eta_s)]^2 J_{eR}^0$	0.165	0.204	0.219	0.095	0.089	0.100	0.130	0.214	0.217
η'_∞ , P	86.8	98.6	117.3	78.6	100.7	139.2	78.7	99.6	108.9
h^*	0.09	0.07	0.05	0.05	0.03				
P/N	15.8	15.8	15.8	15.8	15.8				
ϕ/f_0	1.4	1.45	1.4	1.15	1.15				
$\log \tau_1$	-0.72	-0.61	-0.40	0.00	0.27				
$\log (\bar{M}_v/\bar{M}_w)$	0.10	0.14	0.16	0.07	0.12				
$\log G'_\infty$	4.92	5.03	5.13	4.88	5.18				
$\log (G'_\infty/\nu_2)$	6.69	6.62	6.61	6.72	6.71				

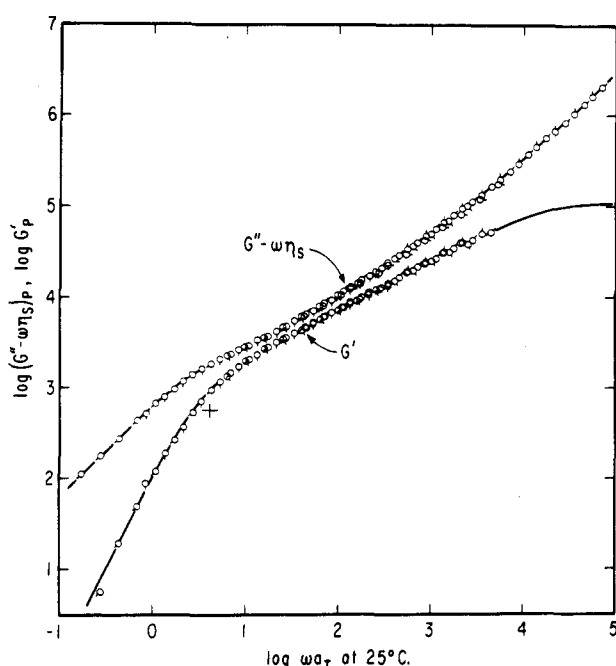


Figure 1. Storage (G'_p) and loss ($(G'' - \omega\eta_s)_p$) moduli, reduced to 25°, plotted logarithmically against frequency for polystyrene LS-13 in Aroclor 1254, concentration 2.69×10^{-2} g/ml. Directions of pips show temperatures of measurement: pip up, 9.3°; 45° clockwise rotations, 14.7, 20.1, 25.0, 30.0, and 35.7°, respectively. Curves drawn according to theory with $N_b = 130$, $h^* = 0.07$, and $(\phi/f_0) = 1.45$.

molecular weight of this sample, compared with LS-13, the terminal zone is shifted to lower frequencies. This results for example in a higher viscosity of the solution at a comparable concentration. An increase in concentration diminishes the spacing between the G' and $G'' - \omega\eta_s$ curves until at high concentrations a crossover region develops in which $G' > G'' - \omega\eta_s$, as shown in Figure 3. In this figure the results are shown for a solution of sample M5E with a concentration of 5.00×10^{-2} g/ml. This behavior has been reported earlier for linear polystyrenes by Holmes et al.⁹ It is associated with the familiar behavior of undiluted polymers, corresponding to a plateau zone in G' , which is attributed to entanglement coupling. The high-frequency pattern remains unaffected as can be seen by comparing Figures 2 and 3.

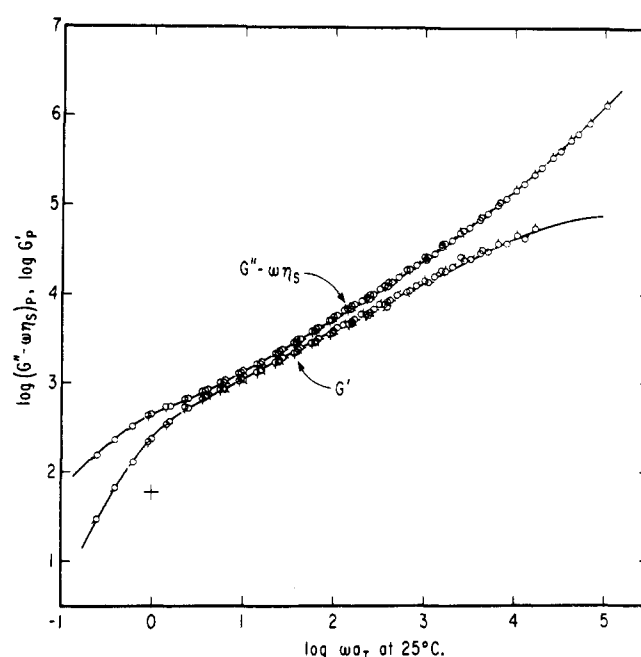


Figure 2. Plots of G'_p and $(G'' - \omega\eta_s)_p$, reduced to 25°, as in Figure 1 for polystyrene M5E in Aroclor 1254, concentration 1.52×10^{-2} g/ml: pip up, 7.2°; 45° clockwise rotations, 13.7, 19.6, 25.1, 30.0, and 34.5°, respectively. Curves are drawn according to theory with $N_b = 338$, $h^* = 0.05$, and $(\phi/f_0) = 1.15$.

Figure 4 shows results for one solution of sample KI-2, 2.73×10^{-2} g/ml. Smooth curves are obtained in which sharp transitions between the different frequency regions are absent. At low enough frequencies, however, a terminal zone is attained at which η and J_e^0 can be determined. At high frequencies the unit slope of $\log (G'' - \omega\eta_s)_p$ against $\log \omega a_T$ again provides for calculation of η'_∞ .

High-Frequency Viscosity. As was shown in I, a useful way of expressing the concentration dependence of η'_∞ is to plot $\log (\eta'_\infty/\eta_s)$ against c , where c is the concentration in grams per milliliter. Figure 5 includes the present results as well as the data in I, obtained on linear samples of polystyrene in the same solvent.

At this stage it may be worthwhile to summarize the different conclusions which can be drawn from this figure: (i) $\log (\eta'_\infty/\eta_s)$ is a linear function of c up to the highest concentration investigated, i.e., 7.6×10^{-2} g/ml; (ii) η'_∞ is in-

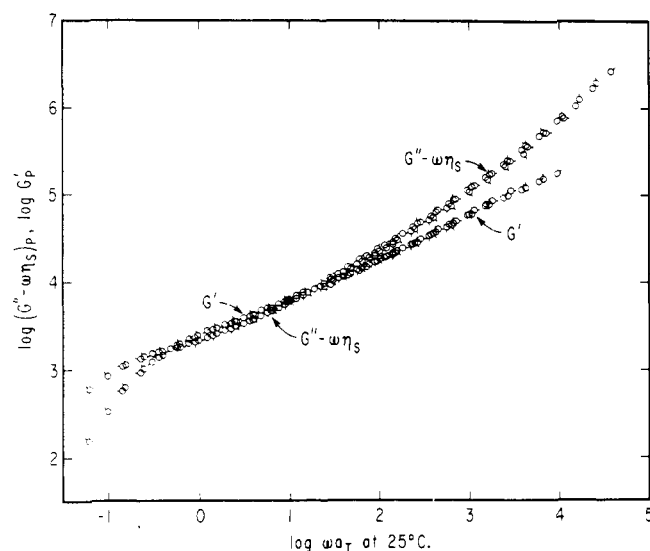


Figure 3. Plots of G'_p and $(G'' - \omega\eta_s)_p$, reduced to 25°, as in Figure 1 for polystyrene M5E in Aroclor 1254, concentration 5.00×10^{-2} g/ml: pip up, 9.8°; 45° clockwise rotations, 14.7, 20.4, 25.0, 30.0, 35.8, 40.2, and 46.0°, respectively.

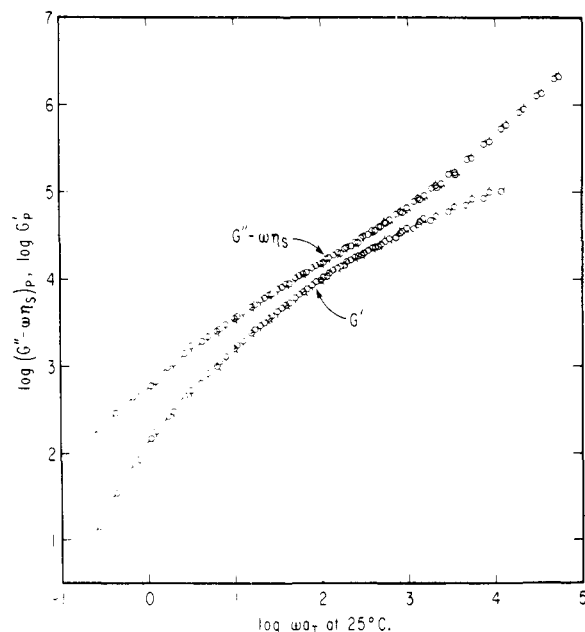


Figure 4. Plots of G'_p and $(G'' - \omega\eta_s)_p$, reduced to 25°, as in Figure 1 for polystyrene KI-2 in Aroclor 1254, concentration 2.73×10^{-2} g/ml: pip up, 9.4°; 45° clockwise rotations, 14.7, 20.2, 24.9, 30.0, and 35.8°, respectively.

dependent of the molecular weight of the polymer within the range covered, as the data for all linear and branched samples fall on the same line; (iii) η'_∞ is also independent of the geometrical structure of the polymer; (iv) the time-temperature superposition can be applied at high frequencies, in spite of large changes in solvent viscosity with temperature. This indicates that the relative viscosity at high frequency, η'_∞/η_s , does not depend on the solvent viscosity for the Aroclor solvents. A measurement made on a solution of a linear sample in Aroclor 1248 falls on the same line as the star samples.

The intrinsic viscosity at high frequency, $[\eta']_\infty$, as obtained from the slope of the line in Figure 5, is 14.3 ml/g, a value already reported in I.

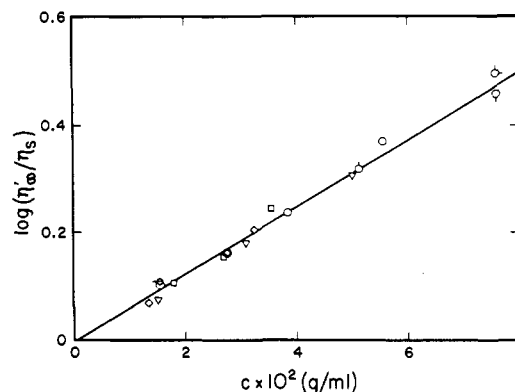


Figure 5. Plot of $\log(\eta'_\infty/\eta_s)$ against concentration for all polystyrene samples investigated. (O) Linear samples, where the pips indicate different molecular weights: no pip, 2.67×10^5 ; up, 8.2×10^4 ; right, 5.1×10^4 ; down, 1.98×10^4 ; and left, 8.6×10^5 . The small circle represents an experiment with Aroclor 1248 ($\eta_s = 2.57$ P at 25°) as solvent: (□) sample LS-13; (▽) sample M5E; (◇) sample KI-2.

Discussion

Low-Frequency Behavior. The infinite dilution viscoelastic properties at low frequencies of the samples investigated here have been studied previously^{8,10,11} with the aid of the Birnboim-Schrag multiple lumped resonator. Although the present data are not accurate enough to allow an extrapolation to infinite dilution, in general the form of the frequency dependence is similar. From the steady flow viscosity η and the steady-state compliance, as given in Table I, another important quantity may be derived, characterizing the linear viscoelastic behavior at low frequencies

$$\left(\frac{\eta}{\eta - \eta_s}\right)^2 J_{eR}^0 = \frac{cRT}{M} \left(\frac{\eta}{\eta - \eta_s}\right)^2 J_e^0 \quad (1)$$

where R is the gas constant and J_{eR}^0 is called the reduced steady-state compliance.⁴ In the limit of zero concentration

$$j_{eR}^0 = \lim_{c \rightarrow 0} \left(\frac{\eta}{\eta - \eta_s}\right)^2 J_{eR}^0 = S_2/S_1^2 \quad (2)$$

where j_{eR}^0 is the intrinsic reduced steady-state compliance. According to the Zimm-Kilb¹² theory for star polymers with f arms the quantities S_1 and S_2 are defined by

$$S_i = (f - 1) \sum_{p=1}^{2N_b-1} (\tau_p/\tau_1)^i + \sum_{p=2}^{2N_b} (\tau_p/\tau_1)^i \quad (3)$$

odd even

$i = 1, 2$

where τ_p are the individual relaxation times and τ_1 the longest one; N_b is the number of subchains per arm. (Note that in ref 6, eq 6 and 7, the ranges of the summations are incorrectly designated.)

Values of $[\eta/(\eta - \eta_s)]^2 J_{eR}^0$, obtained according to eq 1, are given in Table I. They are slightly higher than the values of j_{eR}^0 obtained by Mitsuda^{8,10,11} from infinite dilution data. The difference may be attributed to the higher concentrations and the greater solvent power in the present investigation. Both tend to increase¹³ the value of $[\eta/(\eta - \eta_s)]^2 J_{eR}^0$. With increasing branching, j_{eR}^0 is predicted to decrease rapidly and this behavior has been confirmed experimentally.¹⁴ The present data on $[\eta/(\eta - \eta_s)]^2 J_{eR}^0$ for the 4- and 9-arm stars in Table I show the same trend.

High-Frequency Behavior. The data at high frequencies are consistent with the expectation that short-range internal dynamics of the polymer chains are involved. The

observed concentration dependence of η'_∞ is expected if the viscosity increment due to one element corresponds to a constant relative amount, independent of the length or the type of branching of the whole chain.

Considerable theoretical work has been done recently to seek the origins of this high-frequency behavior. Probably the most likely sources, all of which are ignored in the Rouse-Zimm treatment of chain dynamics, are: (i) frequency-dependent hydrodynamic interaction which cannot be replaced by its equilibrium average; (ii) excluded volume effects; (iii) the effect of chain stiffness on extensibility (real chains with constant bond lengths and bond angles are not satisfactorily approximated by an infinitely extensible ideally flexible subchain model); (iv) the influence of chain structure characterized by internal viscosity, which accounts for an additional energy loss not included in the subchain model.

In connection with (iii), various theories like those of Kirkwood and Auer¹⁵ and of Cerf and Scheraga^{16,17} which are based on stiff rodlike models provide an infinite frequency dynamic viscosity higher than that of the solvent. The study of Warner¹⁸ on finitely extensible dumbbells shows that the incorporation of non-Hookean springs in these models results in the appearance of an infinite-frequency contribution to the dynamic viscosity. According to Bird et al.¹⁹ and Hassager²⁰ the latter is a characteristic feature of approximating a macromolecule by a bead-rod type model as opposed to a Rouse-Zimm type bead-spring model.

Fixman and Kovac,²¹ Nakajima et al.,²² and Edwards and Freed²³ studied the effects of the introduction of constraints of constant bond lengths and constant bond angles in model theories. They show in general that the intrinsic viscosity at high frequency must be independent of the molecular weight of the polymer. This agrees with our experimental observations. The elaborate work of Fixman and Kovac²¹ on a freely jointed linear bead-rod model predicts frequency dependence of the moduli G' and G'' which agrees fairly well with the general behavior observed on linear samples.^{2,3} However, a comparison of some of their preliminary results with data on an appropriate sample of linear polystyrene shows that their treatment still slightly underestimates the infinite-frequency viscosity. Probably this can be improved if a model incorporating constraints on bond angles as well as on bond lengths is treated. This has already been shown by Hassager²⁰ for the relatively simple case of three beads connected by two rigid rods.

In I it was shown that the experimental data on the linear samples could be fitted by the Thurston-Peterlin formulation²⁴ of the Peterlin theory²⁵ which incorporates internal viscosity into the Rouse-Zimm theory. In view of this, an attempt was made to modify the Peterlin theory in order to make it applicable to star polymers. Bazúa and Williams²⁶ recently modified the Peterlin theory; however, especially for small amplitude oscillatory flow, the differences between the treatments are surprisingly minor, so we may safely use the original Peterlin formulation. In essentially the same way as was done by Peterlin with the Rouse-Zimm theory, the Zimm-Kilb theory for star polymers¹² may be modified to include the effect of internal viscosity. This results in the following relations (eq 4 and 5) for the storage and loss moduli for solutions of star polymers with f arms and N_b submolecules per arm, where τ_p is the p th relaxation time given by eq 6. Here f_0 is the friction coefficient of a bead and $\kappa = 3kT/b^2$, i.e., the spring constant (b^2 being the mean square end-to-end distance of the subchain). The quantity λ_p is the p th eigenvalue of the $\mathbf{H}\cdot\mathbf{A}$ matrix defined in the Zimm-Kilb paper. In eq 4 and 5,

$$G' = (cRT/M)\omega^2 \times \left\{ (f-1) \sum_{\substack{p=1 \\ \text{odd}}}^{2N_b-1} \frac{\tau_p^2}{1 + (\omega\tau_p)^2(1+B_p)^2} + \sum_{\substack{p=2 \\ \text{even}}}^{2N_b} \frac{\tau_p^2}{1 + (\omega\tau_p)^2(1+B_p)^2} \right\} \quad (4)$$

$$G'' = \omega\eta_s = (cRT/M)\omega \left\{ (f-1) \sum_{\substack{p=1 \\ \text{odd}}}^{2N_b-1} \frac{\tau_p[1 + (\omega\tau_p)^2(1+B_p)B_p]}{1 + (\omega\tau_p)^2(1+B_p)^2} + \sum_{\substack{p=2 \\ \text{even}}}^{2N_b} \frac{\tau_p[1 + (\omega\tau_p)^2(1+B_p)B_p]}{1 + (\omega\tau_p)^2(1+B_p)^2} \right\} \quad (5)$$

$$\tau_p = f_0/2\kappa\lambda_p \quad (6)$$

B_p describes the influence of internal viscosity (eq 7),

$$B_p = \nu_p \frac{\varphi}{f_0} \left(\frac{p}{2N_b} \right) \quad p = \text{odd} \\ = \nu_b \frac{\varphi}{f_0} \left(\frac{[f-1]p}{2N_b} \right) \quad p = \text{even} \quad (7)$$

where the eigenvalues ν_p are the ratios of λ_p to a set of eigenvalues μ_p and are unity for the free-draining case; φ is an internal viscosity parameter. Following Thurston and Peterlin,²⁴ the μ_p may to a first approximation be put equal to the λ_p of the free-draining molecule: $\lambda_p(0)$. Under this condition

$$\nu_p = \lambda_p(h^*)/\lambda_p(0) \quad (8)$$

where h^* is the reduced hydrodynamic interaction parameter ($= h/N^{1/2}$, where h is the hydrodynamic interaction parameter of the Zimm-Kilb theory and $N = fN_b$, the total number of subchains in the whole star molecule). The ratio φ/f_0 may be treated as a characteristic parameter of the polymer molecule. It is zero in the case of the absence of internal viscosity and increases as the latter increases.

Considering the nature of the normal modes in a star-shaped molecule, one intuitively arrives at the conclusion that the internal viscosity factors B_p should be weighted differently for even and odd normal modes. According to the Zimm-Kilb theory, for even normal modes the motions of all branches of the molecule are coupled, while for odd normal modes the motions of branches are decoupled. This explains why odd normal modes give a $(f-1)$ times degenerate contribution to G' and G'' . In the case of $f=2$, a linear molecule, the above equations become identical with those of the original Peterlin theory. At high frequencies the form of the equation for G'' becomes similar to that for a linear molecule, indicating that the specific differences between the behavior of branched and linear polymers vanish at those frequencies.

The data on the 4-arm star and the 9-arm star (except on the solution with the crossover, Figure 3) were fitted to the above given equations. The parameters needed to describe the shape and the spacing of the curves are the finite number of submolecules per arm N_b , the hydrodynamic interaction parameter h^* , and the ratio φ/f_0 . The choice of N_b has to be made primarily on the basis of the assumption that P/N (the number of monomer units per subchain, P being the degree of polymerization) should be equal for lin-

Table II
Revised³ Parameters at Low and High Frequency, Reduced to 25°, for Linear Polystyrenes in Aroclor 1254

	Sample								
	2a	7a	S102	S102	S108	S108	S108	S108	6a ^a
$\bar{M}_w \times 10^{-3}$	19.8	51	82	82	267	267	267	267	860
$c \times 10^2$, g/ml	7.57	7.56	5.09	7.57	1.53	2.74	3.83	5.54	1.52
η , P	358	660	455	980	270	440	700	1410	19.8
$\log J_e^0$	-5.96	-5.19	-4.87	-4.62	-3.97	-4.15	-4.06	-4.11	-3.19
η'_∞ , P	200	218	146	218	88.6	102	120	163.5	3.28
h^*	0.22	0.20	0.21	0.20	0.19	0.15	0.12	0.08	0.09
P/N	15.8	15.8	15.8	15.8	15.8	15.8	15.8	15.8	15.8
ϕ/f_0	5.0	3.0	2.6	2.0	2.4	2.0	1.8	1.7	2.0
$\log \tau_1$	-3.06	-2.08	-1.87	-1.54	-1.28	-1.10	-0.85	-0.65	-0.54
$\log (\bar{M}_w/\bar{M}_n)$	-0.22	0.02	0.07	0.16	0.05	0.11	0.20	0.21	0.18
$\log G'_\infty$	5.46	5.44	5.29	5.42	4.80	5.02	5.12	5.28	4.71
$\log (G'_\infty/\nu_2)$	6.60	6.58	6.60	6.56	6.64	6.60	6.56	6.56	6.65

^a Results in Aroclor 1248 ($\eta_s = 2.57$ P at 25°).

ear and star-shaped polystyrenes. In paper I the comparisons of theoretical predictions and experimental data were made on the basis of computations with approximate eigenvalues.²⁷ More recently Thurston and Morrison²⁸ and Lodge and Wu²⁹ have shown that the use of exact eigenvalues leads to appreciably different values for N , h^* , and possibly also for ϕ/f_0 . A value of $P/N = 15.8$ was chosen so as to agree with recent data on oscillatory flow birefringence³⁰ which were fitted to the Peterlin theory using exact eigenvalues. The parameters needed for fitting the star data with the aid of exact eigenvalues⁶ are given in Table I.

In order to compare the present results with the linear samples the measurements reported in paper I³ were refitted to the Peterlin theory using exact eigenvalues. The parameters used are given in Table II. A comparison of these data with the former ones in Table I of paper I shows that more realistic values of h^* are obtained; h^* approaches a value of 0.21 at low concentrations and low molecular weights, a value close to but lower than the nondraining limit of 0.25. This is in contrast with rather unrealistic values of h^* of 0.30 and 0.40 needed to fit the data with inexact eigenvalues. Curiously, rather high values of ϕ/f_0 are obtained for the low molecular weight samples, the significance of which is still unknown.

The curves drawn from eq 4 and 5 fit the data over the whole frequency range, as shown in Figures 1 and 2. The values of ϕ/f_0 are somewhat smaller than those obtained for the highest molecular weight linear samples. The calculated magnitudes of G' and G'' have been adjusted slightly as indicated by the position of the crosses in Figures 1 and 2, whose ordinates correspond to $G_+ = cRT/M$ in the theory. The experimental value of G_+ corresponds to a molecular weight \bar{M}_{ve} which is slightly higher than the actual molecular weight, as found also for linear polymers. However, this is simply a concentration effect, and as the concentration decreases \bar{M}_{ve}/\bar{M}_w goes to unity as seen in Tables I and II. The position of the curves along the frequency scale is determined by the magnitudes of the relaxation times in the solvent used. In particular the longest relaxation time τ_1 may be obtained from matching the theoretical and experimental curves along the frequency axis. Its values are given in Tables I and II also.

As one can deduce from Figures 1 and 2, the Peterlin theory provides us with a means of extrapolation to obtain limiting high-frequency values of G' . The values of G'_∞ obtained in this way are given in Tables I and II. The ratio of G'_∞/ν_2 , where ν_2 is the volume fraction of the polymer, ap-

pears to be nearly constant for the linear as well as for the star-shaped polystyrene samples: $\log (G'_\infty/\nu_2) = 6.6 \pm 0.1$. No significant influence of concentration or branching on this quantity can be observed. Although G'_∞ cannot be measured directly because of relatively large errors encountered with the present technique if $G' < 0.1 \times G''$, in principle G'_∞ can also be derived from an integration of G'' data² by means of the equation

$$G'_\infty = \frac{2}{\pi} \int_{-\infty}^{\infty} \omega(\eta' - \eta'_\infty) d \ln \omega \quad (9)$$

where $\eta' = G''/\omega$ is the real part of the dynamic viscosity of the solution. In practice, very high precision is required for η' in the vicinity of η'_∞ in order to evaluate the integral. Actually, only for the data shown in Figure 1 did this method appear to be sufficiently accurate. A planimetric integration of the appropriate graph provided $\log G'_\infty = 4.98 \pm 0.10$, which agrees with the result from the Peterlin theory. It should be stated, however, that G'_∞ is the only quantity in the Peterlin theory which depends on the number of monomer units per subchain P/N . For a slightly different choice of P/N one can obtain theoretical curves which fit the data as well by small changes in the values of h^* and ϕ/f_0 . The value of G'_∞ is a direct function of the value of P/N , which in terms of the Peterlin theory plays the role of an adjustable parameter. This may explain differences in G'_∞ as obtained by different methods.

Some direct measurements of G'_∞ by Plazek et al.³¹ by analysis of creep data on a 1.25% solution of linear polystyrene 6a in tricresyl phosphate showed a value of $\log G'_\infty = 4.56$ compared with a value of 4.71 shown in Table II for a solution of the same polymer in Aroclor 1248 with about the same concentration. This agreement is satisfactory considering the fact that different solvents were used in both investigations.

Acknowledgment. This work was supported in part by grants from the Army Research Office-Durham and the National Science Foundation. We are indebted to Miss Hsin Huang for help with calculations. J.W.M.N. is grateful to the Netherlands Organisation of the Advancement of Pure Research (Z.W.O.) for receiving a travel grant.

References and Notes

- (1) This investigation was part of the research program of the Rheology Research Center, University of Wisconsin.
- (2) D. J. Massa, Ph.D. Thesis, University of Wisconsin, 1970; D. J. Massa, J. L. Schrag, and J. D. Ferry, *Macromolecules*, **4**, 210 (1971).

- (3) K. Osaki and J. L. Schrag, *Polym. J.*, **2**, 541 (1971).
- (4) J. D. Ferry, "Viscoelastic Properties of Polymers", 2nd ed, Wiley, New York, N.Y., 1970.
- (5) D. J. Massa and J. L. Schrag, *J. Polym. Sci., Part A-2*, **10**, 71 (1972).
- (6) K. Osaki and J. L. Schrag, *J. Polym. Sci., Polym. Phys. Ed.*, **11**, 549 (1973).
- (7) K. Osaki, Y. Mitsuda, R. M. Johnson, J. L. Schrag, and J. D. Ferry, *Macromolecules*, **5**, 17 (1972).
- (8) Y. Mitsuda, K. Osaki, J. L. Schrag, and J. D. Ferry, *Polym. J.*, **4**, 24 (1973).
- (9) L. A. Holmes, S. Kusamizu, K. Osaki, and J. D. Ferry, *J. Polym. Sci., Part A-2*, **9**, 2009 (1971).
- (10) Y. Mitsuda, Ph.D. Thesis, University of Wisconsin, 1973.
- (11) Y. Mitsuda, J. L. Schrag, and J. D. Ferry, *Polym. J.*, **4**, 668 (1973).
- (12) B. H. Zimm and R. W. Kilb, *J. Polym. Sci.*, **37**, 19 (1959).
- (13) H. Janeschitz-Kriegl, *Adv. Polym. Sci.*, **6**, 170 (1969).
- (14) Y. Mitsuda, J. L. Schrag, and J. D. Ferry, *J. Appl. Polym. Sci.*, **18**, 193 (1974).
- (15) J. G. Kirkwood and P. L. Auer, *J. Chem. Phys.*, **19**, 281 (1951).
- (16) R. Cerf, *C. R. Hebd. Seances Acad. Sci.*, **234**, 1549 (1952).
- (17) H. A. Scheraga, *J. Chem. Phys.*, **23**, 1526 (1955).
- (18) H. R. Warner, Jr., *Ind. Eng. Chem., Fundam.*, **11**, 379 (1972).
- (19) R. B. Bird, H. R. Warner, Jr., and D. C. Evans, *Adv. Polym. Sci.*, **8**, 1 (1971).
- (20) O. Hassager, *J. Chem. Phys.*, **60**, 2111, 4001 (1974).
- (21) M. Fixman and J. Kovac, *J. Chem. Phys.*, **61**, 4939, 4950 (1974).
- (22) H. Nakajima, M. Doi, K. Okano, and Y. Wada, *Rep. Prog. Polym. Phys. Jpn.*, **16**, 91 (1973).
- (23) S. F. Edwards and K. F. Freed, *J. Chem. Phys.*, **61**, 1189 (1974).
- (24) G. B. Thurston and A. Peterlin, *J. Chem. Phys.*, **46**, 4881 (1967).
- (25) A. Peterlin, *Kolloid Z. Z. Polym.*, **209**, 181 (1966); *J. Polym. Sci., Part A-2*, **5**, 179 (1967).
- (26) E. R. Bazúa and M. C. Williams, *J. Polym. Sci., Polym. Phys. Ed.*, **12**, 825 (1974).
- (27) C. W. Pyun and M. Fixman, *J. Chem. Phys.*, **42**, 3838 (1965).
- (28) G. B. Thurston and J. D. Morrison, *Polymer*, **10**, 421 (1969).
- (29) A. S. Lodge and Yeen-Jing Wu, MRC Technical Summary Report No. 1250, Mathematics Research Center, University of Wisconsin, Madison, Wisconsin, 1972.
- (30) J. W. Miller and J. L. Schrag, *Macromolecules*, **8**, 361 (1975).
- (31) E. Riande, H. Markovitz, D. J. Plazek, and N. Raghupathi, private communication.

Sequence Distribution–Glass Transition Effects in Copolymers of Vinyl Chloride and Vinylidene Chloride with Methyl Acrylate

Alan E. Tonelli

Bell Laboratories, Murray Hill, New Jersey 07974. Received January 23, 1975

ABSTRACT: The conformational entropies of copolymer chains are calculated through utilization of semiempirical potential energy functions and adoption of the rotational isomeric state model of polymers. It is assumed that the glass transition temperature, T_{gp} , is inversely related to the intramolecular, equilibrium flexibility of a copolymer chain as manifested by its conformational entropy. If, for example, the conformational entropy of a 50:50 copolymer of A and B monomer units is larger (smaller) than half the sum of the entropies of the two homopolymer chains (poly-A and poly-B), then the copolymer T_{gp} should be lower (higher) than that predicted by bulk additive relations such as the Fox equation. This approach is applied to the vinyl copolymers of vinyl chloride and vinylidene chloride with methyl acrylate, where the stereoregularity of each copolymer is explicitly considered, and correctly predicts the observed deviations from the Fox relation when they occur. It therefore appears that the sequence distribution– T_g effects observed in many copolymers may have an intramolecular origin in the form of specific molecular interactions between adjacent monomer units, which can be characterized by estimating the resultant conformational entropy.

It has recently been suggested¹ that the frequently observed^{2–7} sequence distribution dependent deviations of the glass transition temperatures T_{gp} of copolymers away from the values predicted by simple bulk additive relations, such as the Fox equation⁸ [$1/T_{gp} = (W_A/T_{gA}) + (W_B/T_{gB})$, where W_A and W_B and T_{gA} and T_{gB} are the weight fractions of the comonomer units A and B and the glass transition temperatures of their homopolymers, respectively], may have their origins in specific intrachain interactions. The conformational entropy was calculated and employed as a measure of the equilibrium flexibility of a copolymer chain, and an inverse relation between T_{gp} and copolymer flexibility was assumed. If, for example, the conformational entropy of a 50:50 copolymer of A and B monomer units is larger (smaller) than half the sum of the entropies of the two homopolymer chains (poly-A and poly-B), then the copolymer T_{gp} is expected to be lower (higher) than that predicted by bulk additive relations such as the Fox equation.

This approach was applied¹ to the copolymers of styrene and α -methylstyrene with acrylonitrile and was successful in predicting the sequence distribution dependent deviations from the Fox equation observed^{2,4,7} for these two copolymers. In the present work we extend the previously proposed¹ correlation of conformational entropy with T_{gp}

to the copolymers of vinyl chloride (VC) and vinylidene chloride (VDC) with methyl acrylate (MA).

Calculation of Homo- and Copolymer Chain Entropies

Adoption of the rotational isomeric state (RIS) model⁹ of polymer chains permits the utilization of matrix multiplication methods¹⁰ to evaluate the conformational entropy¹¹ S of a polymer chain of n bonds

$$S = R \ln z + \frac{RT}{z} \left(\frac{dz}{dT} \right) \quad (1)$$

$$z = J^* \left[\prod_{i=2}^{n-1} U_i \right] J \quad (2)$$

$$J^* = [100 \dots 0](1 \times \nu); J = \begin{bmatrix} 1 \\ 1 \\ 1 \\ \vdots \\ 1 \end{bmatrix} (\nu \times 1) \quad (3)$$

where the $\nu \times \nu$ (ν rotational states assumed about each backbone bond) statistical weight matrix for bond i